Photochemical Generation of Light Responsive Surfaces

Eva Blasco, Milagros Piñol, Luis Oriol, Bernhard V. K. J. Schmidt, Alexander Welle, Vanessa Trouillet, Michael Bruns, and Christopher Barner-Kowollik**

The preparation of patterned photoswitchable surfaces by employing the nitrile imine-mediated tetrazole ene cycloaddition (NITEC) photoinduced reaction in the presence of dipolarophiles based on photoresponsive azobenzene moieties is reported. The dipolarophile used is a maleimide carrying either an azobenzene unit or a first generation dendron containing two azobenzene units. X-ray photoelectron spectroscopy (XPS) is employed to analyze the functionalized silicon wafers, while time-of-flight secondary ion mass spectrometry (ToF-SIMS) evidences the spatial control of the functionalization of the surface achieved by using a micropatterned shadow mask. Water contact angle measurements and optical inspection observing the behavior of a water droplet demonstrate the photoinduced change on wettability of the structured functionalized surfaces due to the reversible *trans*-to-*cis* isomerization of the azobenzene moities.

1. Introduction

Responsive smart surfaces have recently attracted significant attention because of the associated interesting applications such as biosensors, intelligent membranes or microfluidic devices.[1–3] The incorporation of photoresponsive molecules onto variable surfaces makes the study of such systems even more attractive as the properties of the surfaces can be controlled by light as an external and remote stimulus. Due to a rapid, reversible and high quantum yield *trans*-to-*cis* photoisomerization, azobenzenes are one of the best candidates for photoresponsive surface design. The thermodynamically more stable *trans*-isomer can be photoisomerized to the *cis*-isomer, which can be reverted again to the *trans* form either photochemically or via a thermal stimulus. *Trans*-to-*cis* isomerization results in an increase in the dipole moment of the molecule giving the possibility to prepare surfaces with photocontrolled wettability. *Trans*-azobenzene features a dipolar moment close to zero while the *cis*-isomer has a dipole moment around 3 D.[4,5] Moreover, by simple substitution with different groups in 4- and 4′- positions of the azobenzene unit it is possible to modulate the dipole moment offering a broad range of possibilities in the system design.[6,7]

Pioneering studies on photoresponsive surfaces were reported by Ichimura and co-workers using a flat surface modified with a calix[4]resorcinarene containing four pendant azobenzene units that was irradiated with a gradient in light intensity achieving the light-driven motion of liquids.[4,8] Selected examples in compact monolayers containing azobenzene moieties prepared on silicon substrates were described by Delorme as well as Hamelmann et al.[9,10] These photoresponsive surfaces were prepared either by covalent grafting of azobenzene moieties onto an isocyanate-functionalized monolayer or direct grafting of silane-containing azobenzene. Recently, efficient photoresponsive rough surfaces fabricated via layer-by-layer deposition were also reported. For example, Liu et al. prepared a surface switchable between slippery and sticky states when the azo-compound assumes *trans* or *cis* configuration.[11] The coating consists of silicon elastomer containing trifluoromethoxy-azobenzene moieties. Lim et al. also prepared fluorinated azobenzene-modified nanoporous substrates.[12] Upon UV irradiation, the surface was reversibly switched between superhydrophobic and superhydrophilic states. Standard approaches such as Langmuir-Blodgett[13,14] or spin-coated films[15–17] can also be applied to produce azobenzene-functionalized thin films. In the present work, however, we are focusing on a photochemically driven covalent attachment of the photoresponsive moiety onto an inorganic surface. A powerful method for modifying surfaces is click chemistry,[18] a chemical design philosophy featuring reactions with (ideally) quantitative yield, orthogonal reactivity, stereospecificity and high atom economy.[19] Very recently light

E. Blasco, Dr. M. Piñol, Dr. L. Oriol
Instituto de Ciencia de Materiales de Aragón (ICMA)
Universidad de Zaragoza-CSIC
Departamento de Química Orgánica
Facultad de Ciencias
50009 Zaragoza, Spain
E-mail: loriol@unizar.es

B. V. K. J. Schmidt, Prof. C. Barner-Kowollik
Preparative Macromolecular Chemistry
Institut für Technische Chemie und Polymerchemie
Karlsruhe Institute of Technology (KIT)
76128 Karlsruhe, and Soft Matter Synthesis Laboratory
Institute for Biological Interfaces (IBG I)
Karlsruhe Institute of Technology (KIT)
76344 Eggenstein-Leopoldshafen, Germany
E-mail: christopher.barner-kowollik@kit.edu

Dr. A. Welle
Institute for Biological Interfaces (IBG I)
Karlsruhe Institute of Technology (KIT)
76344 Eggenstein-Leopoldshafen, Germany

V. Trouillet, Dr. M. Bruns
Institute for Applied Materials (IAM-ESS) and Karlsruhe Nano Micro Facility (KNMF), Karlsruhe Institute of Technology (KIT)
76344 Eggenstein-Leopoldshafen, Germany

DOI: 10.1002/adfm.201203602

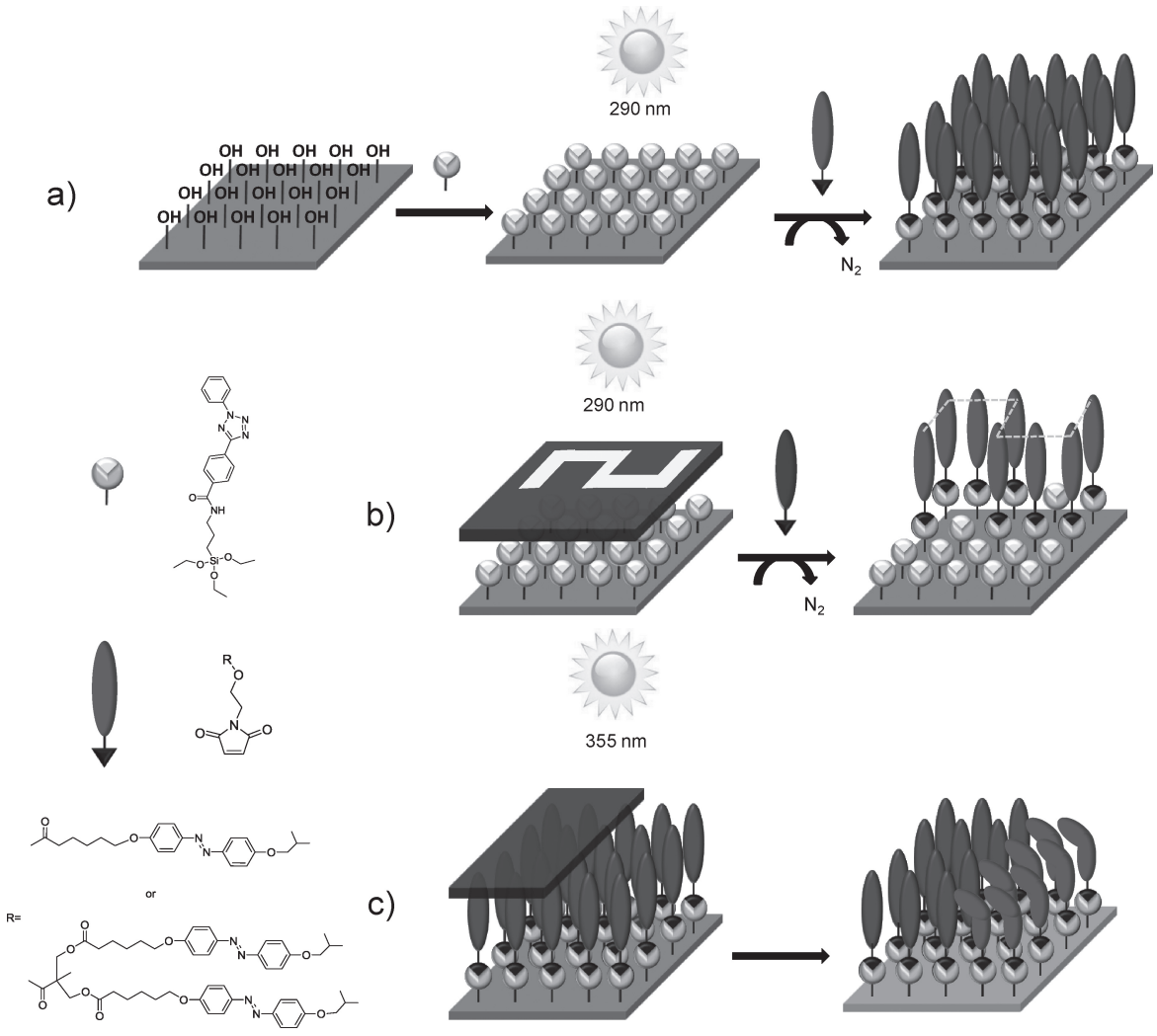

Scheme 1. a) Azobenzene-functionalization of surfaces via the NITEC approach. b) Azobenzene-functionalization of surfaces with spatial control employing a micropatterned shadow mask. c) Partial photoisomerization of an azobenzene-functionalized surface employing a shadow mask covering half of the surface.

triggered click conjugations were applied to surfaces providing the opportunity to achieve spatial control leading to new possibilities for the generation of nanostructured materials.[20–22]

The utilization of UV initiated reactions such as the nitrile imine-mediated 1,3-dipolar cycloaddition of a tetrazole and an ene (NITEC) represents a powerful photochemically driven ligation protocol. The NITEC reaction was firstly reported by Huisgen and Sustmann in 1967[23] and recently significantly expanded by Lin and co-workers.[24] In previous work, we have also successfully employed the NITEC strategy for ambient temperature grafting of polymers onto variable surfaces such as silicon or cellulose.[21] The NITEC reaction proceeds via the generation of a nitrile imine dipole by irradiation with UV light of a tetrazole compound and the release of nitrogen. The nitrile imine intermediate is able to react spontaneously with a large variety of alkenes forming a pyrazoline cycloadduct in near quantitative yields.[24,25]

In the current work, we report the preparation and study of responsive surfaces using exclusively light as stimulus for both the preparation of azobenzene-modified surfaces and the subsequent control of the surface properties via UV light. By employing the NITEC approach using azobenzene dipolarophiles, spatially controlled photoresponsive surfaces can be prepared (see **Scheme 1** for an overview of the applied synthetic strategy). These dipolarophiles are a maleimide containing either a single azobenzene moiety or a first-generation dendron carrying two azobenzene units. Initially, the NITEC reaction between the photoresponsive dipolarophiles and a model tetrazole was assessed in solution and subsequently adopted for surface grafting. Two powerful surface analysis techniques have been utilized to evidence the surface grafting, i.e., X-ray photoelectron spectroscopy (XPS) and time-of-flight secondary ion mass spectrometry (ToF-SIMS). In addition, water contact-angle measurements and visual inspection evidenced by the provided movies (refer to Supporting Information), demonstrate the photocontrolled tunable wettability of the surface by azobenzene photoisomerization.

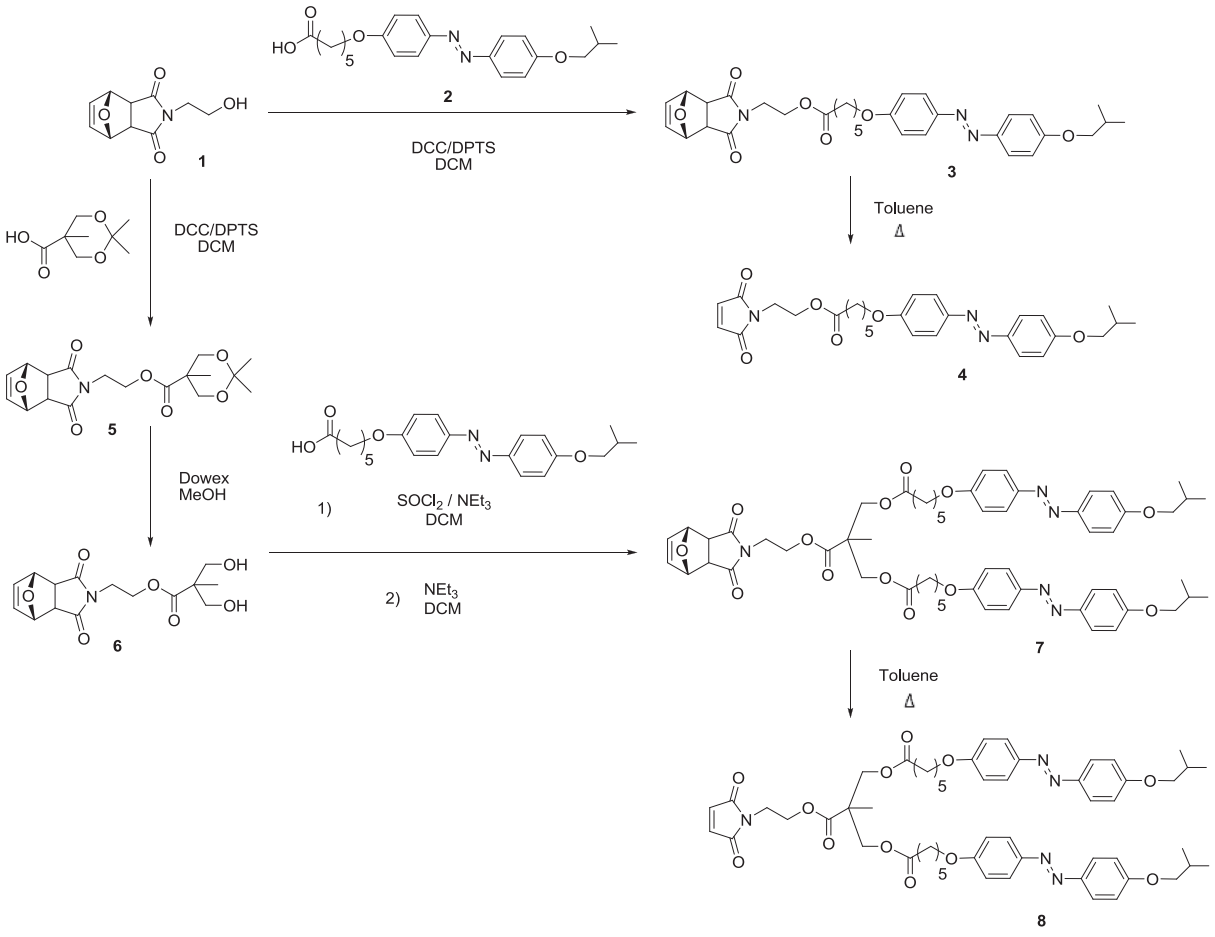

Scheme 2. Synthesis of the maleimide-containing azobenzene derivates.

2. Results and Discussion

2.1. Synthesis

In the current study, the tetrazole-functionalized silane and maleimide-containing azobenzenes (**4**) and (**8**) were prepared for subsequent surface functionalization. For the synthesis of the tetrazole, a previously reported procedure was employed.[21] In the case of the maleimide-containing azobenzene derivates (**4**) and (**8**) (**Scheme 2**), alkoxy groups were introduced in the 4- and 4′- positions of the azobenzene core in order to increase the difference in polarity between *trans*- (apolar) and *cis*- (polar) isomers under irradiation.[26] The maleimide-containing azobenzene (**3**) was prepared by esterification of a protected maleimide containing a hydroxyl group (**1**) with the azobenzene (**2**). On the other hand, a protected maleimide-containing 2,2-dihydroxymethylpropionic acid derivate (**6**) was synthesized and esterified with the acid chloride derivate of (**2**). Finally, the intermediates (**3**) and (**7**) were readily deprotected by a heat induced retro-Diels-Alder reaction in quantitative yields. Synthetic details are depicted in Scheme 2, the Experimental Section and the Supporting Information (Figure S1 and S2).

2.2. Solution Tests

As noted above, the NITEC approach is a very efficient light triggered ligation technique for both small molecules and macromolecular conjugation.[21,23–25,27] However, the NITEC UV- initiated reaction has not been employed before for the preparation of photoresponsive surfaces using chromophores with a strong absorption in the UV region such as azobenzenes. Before applying the NITEC approach to link azobenzene moieties to the surface, solution experiments were developed to evaluate reaction conditions as well as conjugation efficiencies. The reaction between the tetrazole functionalized silane (**9**) and an excess of maleimide-containing azobenzene (**4**) was carried out in dichloromethane (DCM) (**Scheme 3**). Electrospray ionization coupled to mass spectrometry (ESI-MS) was employed to confirm the photoadduct formation. The first parameter assessed was the selection of a suitable wavelength to perform the photoreaction. The tetrazole **(9)** in solution shows an absorption band with the maximum at 280 nm while the *trans*-azobenzene **(4)** presents two absorption bands, a strong one centred at 360 nm attributed to the π–π^* transition and a weak one at about 450 nm corresponding to the n-π^* transition (Figure S3 in the Supporting Information). Following the previously established

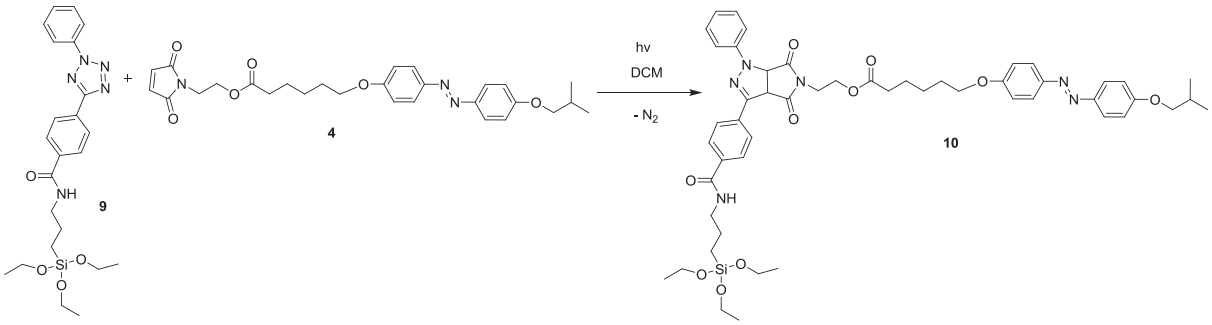

Scheme 3. Tetrazole (**9**) and maleimide-containing azobenzene (**4**) employed in the solution experiments (λ = 290–315 nm).

procedure,[21] the reaction was performed at 254 nm, where both tetrazole and azobenzene present similar absorptions. However, only low conversions were achieved when using a low power light source (6 W) and decomposition of the compounds was detected by ESI-MS using a higher power light source (36 W). In order to improve the efficiency of the NITEC approach, a lamp emitting radiation with the maximum between 290–315 nm (9 W) was employed to avoid the azobenzene absorption band. This time, the formation of the desired adduct (**10**) was confirmed by ESI-MS. Once the successful coupling was confirmed, the reaction times were systematically varied. It was observed that after 20 min at ambient temperature, the targeted coupling product (**10**) was formed (m/z = 949.4 $[M+H]^+$, 971.7 $[M+Na]^+$) and after 40 min almost all tetrazole (m/z = 492.3 $[M+Na]^+$) was reacted. After one hour, only mass to charge ratios corresponding to the azobenzene (**4**) employed in excess (m/z = 530.4 $[M+Na]^+$) and product (**10**) were detected (refer to Figure S4 in the Supporting Information).

2.3. Azobenzene Surface Functionalization

After evidencing the efficiency of the NITEC reaction in the presence of azobenzene in solution, the same reaction was carried out with tetrazole-functionalized silicon wafers (**Scheme 4**). Firstly, the covalent attachment of the tetrazole containing silane was performed in toluene at 50 °C after cleaning and activation of the surfaces (Experimental Section). The tetrazole-functionalized silicon wafer (TET) was rinsed extensively with fresh solvent and sonicated to ensure no physisorbed tetrazole was present on the surface. To graft the maleimide azobenzene molecules to the surface, the NITEC approach was employed by using the optimum wavelength regime between 290 and 315 nm identified in the solution tests. A silicon wafer was placed in a quartz flask containing a maleimide-containing azobenzene (**4**) solution in DCM (7 mM) and was irradiated with the suitable light source (9 W, 290–315 nm) for 2 h. XPS was employed to prove the functionalization of the silicon wafers. In the XPS spectra (**Figure 1**) it is possible to observe intense peaks around 285–290 eV corresponding to C 1s and close to 400–402 eV attributed to N 1s. The main peak in the C 1s at 285.0 eV corresponding to saturated carbon atoms (C–C, C–H) has been used as reference. As reported earlier, peaks at 286.6 eV and 288.5 eV can be assigned to carbon atoms singly bonded with oxygen and nitrogen (C–O, C–N) and the carboxylic group (N/O–C=O), respectively.[28,29] The N 1s spectrum displays a strong peak at 400.2 eV that can be assigned to the tetrazole species[30] or azo group and a weak one at 402.7 eV that probably correspond to positively charged nitrogen.[31]

The relative intensities of the signals was calculated by normalizing to the (C–O, C–N) intensity (Figure S5 and S6 in the Supporting Information). As expected, in comparison with TET

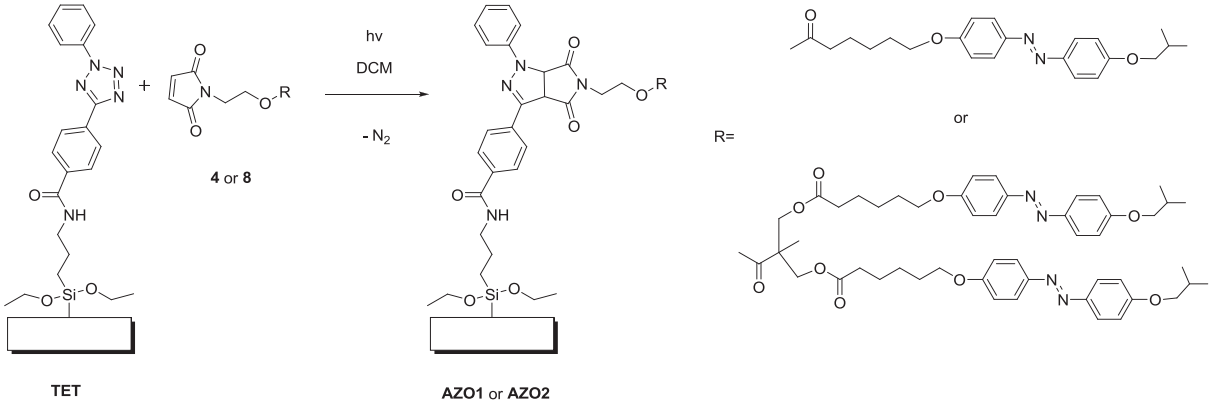

Scheme 4. NITEC reaction between a tetrazole-functionalized surface and the maleimide containing azobenzene derivates (**4**) and (**8**). Only one Si–O has been considered in the scheme, although a mixture of mono-, di-, and tri- attachment might occur.

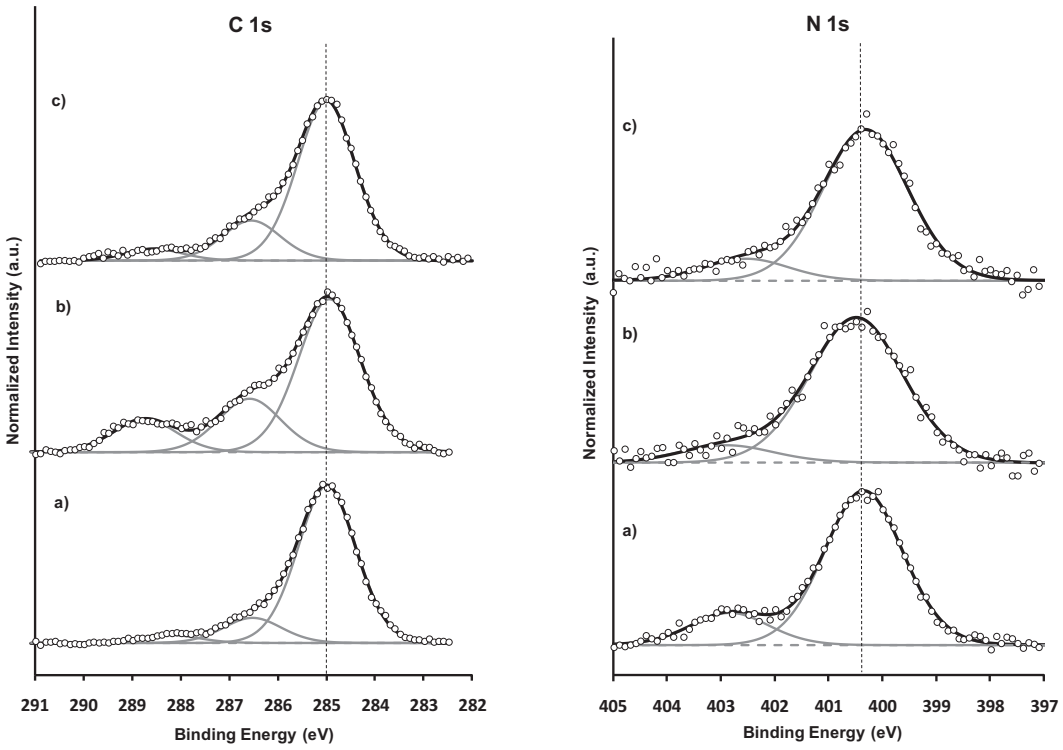

Figure 1. Comparison of the C 1s and N 1s normalized regions of the XPS spectra of a) TET, b) AZO1, and c) AZO2 functionalized silicon wafers.

the N/(C–O, C–N) ratio decreased on the functionalized surface (AZO1) evidencing the presence of azobenzene on the surface. Similarly, the photoligation reaction was carried out with the first-generation azodendron (**8**). A silicon wafer was placed in a quartz flask containing the azocompound (**8**) solution in DCM (3.5 mM) and was irradiated with the same lamp (9 W, 290–315 nm) for 2 h. Following the same procedure, the functionalized silicon wafer (AZO2) was analyzed by XPS. The relative intensities of the signals were calculated by normalizing to C–O, C–N intensity again and it was observed that the N/(C–O, C–N) ratio decreased in comparison with TET (Figure S6 in the Supporting Information). Nevertheless, in this case the experimental result is not in agreement with the theoretical value evidencing incomplete functionalization of the surface. In order to optimize the photoconjugation reaction with compound (**8**), several conditions with different reaction times were assessed. The intensity of the N/(C–O, C–N) ratio was chosen as a sensor for the reaction evolution (Figure S7 in the Supporting Information for further details). The best result was achieved with 6 h reaction time for which a functionalization close to 50% was reached according to the quantitative evaluation of the XPS data. The efficiency loss in the surface photoreaction might be attributed to a higher steric hindrance in the case of the azodendron (**8**) in comparison with the single molecule (**4**).

ToF-SIMS is a surface-sensitive analytical method providing chemical images generated by collecting mass spectra at a high lateral resolution. To evidence spatial control in azobenzene functionalization, a shadow mask containing a micropattern was employed (Scheme 1b). Tetrazole-functionalized surfaces were immersed in an azobenzene solution of both derivates (**4**) and (**8**) and were irradiated with the same a UV source (9 W, 290–315 nm) to perform the reaction with spatial control. **Figure 2** depicts the ToF-SIMS images of the patterned surfaces. $C_{16}H_{17}N_2O_2^-$ (m/z = 269.2), and a second fragment $C_{12}H_8N_2O_2^-$ at 212.1 m/z corresponding to organic fragments of azobenzene evidence the presence of azobenzene exclusively in UV exposed areas, while these peaks were not detected in the non irradiated regions. Both fragments can also be found in ToF-SIMS data of the used azobenzene-containing molecules (**4**) and (**8**) (Figure S8 in the Supporting Information). However, the [M+Na] ion cannot be detected after the photografting step discarding physisorption of the precursor molecules (**4**) and (**8**) and consequently unambiguously evidencing a covalent attachment. ToF-SIMS data of compound (**8**) covalently grafted or physically adsorbed are shown as an example in Figure S9 in the Supporting Information.

2.4. Wettability Study

After evidencing the presence of azobenzene on the surface by XPS and ToF-SIMS, azobenzene *trans*-to-*cis* photoisomerization was provoked by UV irradiation of the surface. For this photoisomerization, a lamp with the maximum emission wavelength close to 355 nm was chosen (the strongest absorption band of *trans*-azobenzene is centered around 360 nm) in order to induce *trans*-to-*cis* isomerization of the azobenzenes. Azobenzene functionalized surfaces (AZO1 and AZO2) were illuminated using a shadow mask covering half of the surface to generate two regions on the surfaces with different

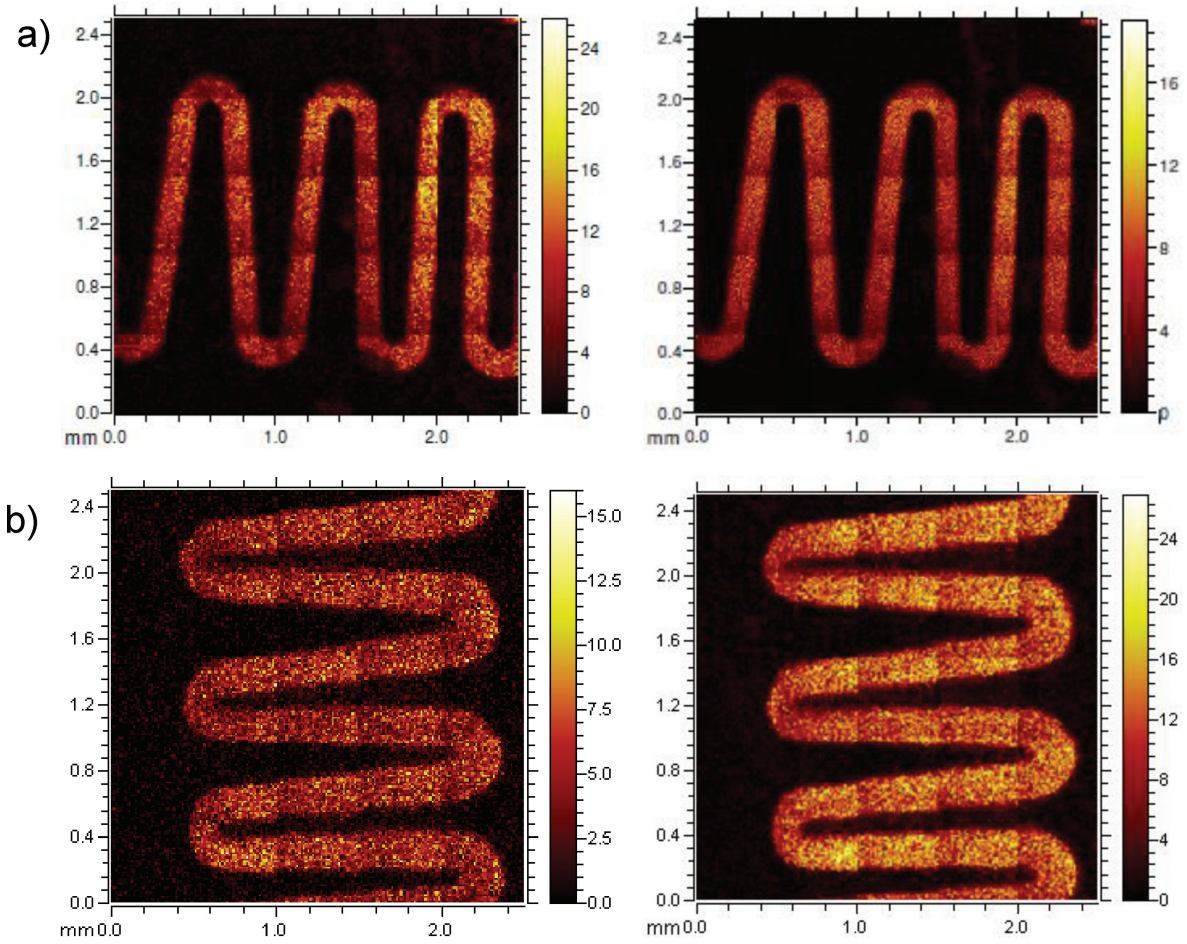

Figure 2. ToF-SIMS images of a) the azobenzene (**4**) and b) azobenzene (**8**) immobilized in a wave pattern defined by the applied photomask. Negative polarity SIMS, 269.1 u and 212.1 u, assigned to $C_{16}H_{17}N_2O_2^-$ (left) and $C_{12}H_8N_2O_2^-$ (right).

polarity due to the photodriven azobenzene isomerization in the exposed areas (Scheme 1c). As noted in the introduction, *trans*-to-*cis* isomerization provokes changes in the dipole moment allowing to tune the surface wettability. A simple and effective technique employed to macroscopically monitor the photoisomerization is via contact angle (CA) measurements. Advancing and receding CAs were determined in non-irradiated (*trans*-azobenzene) and irradiated (*cis*-azobenzene) regions of both surfaces (**Table 1**). On an ideal surface, the advancing and the receding angles will be identical.[32] It is well known that roughness or chemical heterogeneity can cause CA hysteresis, yet it is also reported that even surfaces, which are initially smooth and homogeneous, can exhibit CA hysteresis because of a reorganization of surface molecules.[4,33] In the present case, no significant modification in the advancing CA can be observed. However, a significant change of 15° in receding CA occurred on the azobenzene-functionalized surface (AZO1) evidencing that the photoisomerization occurs and has influence on the wettability of the surface. In the case of azobenzene-functionalized surface (AZO2), smaller differences were detected between the non-irradiated and the irradiated zone were detected, probably due to a more heterogeneous and less azobenzene-functionalized surface being produced. As expected, the CA in the *cis*-azobenzene region in both cases decreased as a consequence of the dipole moment increase. Reported differences in contact angle on *trans* and *cis* azobenzene-functionalized smooth surfaces did not exceed 10°[34,35] whereas higher differences were achieved in the azobenzene-functionalized surface (AZO1).

Visual experiments by using a water droplet were performed to demonstrate the photoswitchable wettability of the functionalized surface. It was evidenced that when azobenzenes linked to the surface adopt the *trans* configuration a water droplet can be slipped over the surface whereas the water droplet is sticky if azobenzenes are in the *cis* configuration. Such a different behavior is more pronounced in the case of surface modified with azobenzene (**4**). For a visual demonstration of the switching effect, please refer to the movies which are contained in the Supporting Information. In these experiments, a water droplet was placed in each region of the surface, irradiated as well as non-irradiated, and it was forced to move over the surface. Reversible *cis* to *trans* thermal isomerization was checked by keeping the surface in the dark for 24 h before evaluating the water droplet behavior again. After 24 h, the water droplet slipped over the entire surface proving that the azobenzene adopted *trans* configuration in both regions. Although the

Table 1. Contact angle measurements of the prepared azo-functional surfaces.

Surface	Advancing angle	Receding angle
AZO1 (non-irradiated)	87.0° ± 1.0°	56.7° ± 3.5°
AZO1 (irradiated)	86.7° ± 1.5°	41.7° ± 1.5°
AZO2 (non-irradiated)	83.0° ± 2.5°	52.3° ± 2.5°
AZO2 (irradiated)	83.5° ± 3.0°	42.3° ± 4.5°

thermal isomerization is slow (hours) it can be readily accelerated by heating or by exposure to visible light.

3. Conclusions

A novel and efficient avenue for the spatial resolved photocontrolled functionalization of surface with azobenzene moieties is reported by employing the NITEC (nitrile imine-mediated tetrazole ene cycloaddition) photoinduced reaction in presence of photoresponsive dipolarophiles. The photoligation reaction in the presence of a molecule featuring a single azobenzene unit and a maleimide group was performed as well as with a first-generation dendron containing two azobenzene groups. The ToF-SIMS images evidence functionalized surfaces in a highly spatial controlled fashion in both cases. Photocontrolled *trans*-to-*cis* azobenzene isomerization of the surface provokes a change in the dipolar moment allowing the tuning of the surface wettability. Visual experiments by using a water droplet demonstrate the photoswitchable wettability. An optimum photoresponse has being achieved when the photoligation is performed with azobenzene (**4**).

4. Experimental Section

Materials: The protected maleimide (**1**) and the tetrazole-functionalized silane (**9**) were prepared according to the procedure previously reported.[36,16b] Experimental details for the synthesis of 6-[4-(4'isobutyloxiphenylazo) phenyloxy]hexanoic acid (**2**) are given in the Supporting Information. All other reagents were purchased from Aldrich and used as received without further purification.

*Synthesis of (***3***)*: The protected maleimide (**1**) (0.4 g, 2.2 mmol), 6-[4-(4′-cyanophenylazo)phenyloxy] hexanoic acid (**2**) (1.0 g, 2.6 mmol) and 4-(dimethylamino)pyridinium 4-toluenesulfonate (DPTS) (0.6 g, 2.2 mmol) were dissolved in dichloromethane (15 mL). The reaction flask was flushed with argon, and *N,N′*-dicyclohexylcarbodiimide (DCC) (0.6 g, 2.8 mmol) was added. The mixture was stirred at ambient temperature for 24 h under argon atmosphere. The white precipitate formed was filtered off, and the solvent was evaporated. The crude product was purified by flash column chromatography on silica gel and eluted with 1:9 ethyl acetate/dichloromethane The target product was obtained as a yellow powdery solid. Yield: 70%. IR (KBr): ν = 1743, 1713 (C=O), 1601, 1580, 1499 (Ar), 1396, 1247 (C-O), 840 (Ar). ^{1}H NMR (400 MHz, $CDCl_3$, δ): 7.90-7.86 (m, 4H, Ar H), 7.07–6.95 (m, 4H, Ar H), 6.50 (t, J = 1.0 Hz, 2H, =C-H), 5.27 (t, J = 1.0 Hz, 2H, CH-O), 4.33–4.19 (t, J = 5.2 Hz, 2H, CH_2-OCO), 4.05 (t, J = 6.4 Hz, 2H, CH_2-OPh), 3.89–3.66 (m, 4H, CH_2-N, CH_2-O), 2.86 (s, 2H, CH), 2.34 (t, J = 7.5 Hz, 2H, CH_2-CO), 2.19-2.09 (m, 1H, CH), 1.88-1.81 (m, 2H, CH_2), 1.74-1.67 (m, 2H, CH_2), 1.64–1.45 (m, 2H, CH_2), 1.07 (d, J = 6.7 Hz, 6H, CH_3) ppm. ^{13}C NMR (100 MHz, $CDCl_3$, δ): 176.0, 173.3 (CO), 161.3, 161.2, 146.9, 146.8 (C4 Ar), 136.5, 124.29, 114.7, 114.6 (=C-H), 80.9 (CH-O), 74.7, 67.9, 60.5 (CH_2-O), 47.4 (CH), 37.9 (CH_2-N), 33.9, 29.7 (CH_2), 28.3 (CH), 25.6, 24.4 (CH_2), 19.3 (CH_3) ppm.

*Synthesis of (***4***)*: The azobenzene (**3**) was suspended in 150 mL toluene and heated to reflux. The reaction was monitored by TLC. After 4 h, the solvent was removed under reduced pressure to give (**4**) as a yellow powder. IR (KBr): ν = 1735, 1707 (C = O), 1601, 1580, 1499 (Ar), 1402, 1242 (C-O), 839 (Ar). Yield: 98%. ^{1}H NMR (400 MHz, $CDCl_3$, δ): 7.90-7.82 (m, 4H, Ar H), 7.04–6.91 (m, 4H, Ar H), 6.71 (s, 2H, =C-H), 4.30–4.19 (t, J = 5.3 Hz, 2H, CH_2-OCO), 4.03 (t, J = 6.4 Hz, 2H, CH_2-OCO), 3.89–3.66 (m, 4H, CH_2-O, CH_2-N), 2.34 (t, J = 7.4 Hz, 2H, CH_2-CO), 2.19-2.09 (m, 1H, CH), 1.90-1.81 (m, 2H, CH), 1.74-1.67 (m, 2H, CH_2), 1.64–1.45 (m, 2H, CH_2), 1.07 (d, J = 6.7 Hz, 6H, CH_3) ppm. ^{13}C NMR (100 MHz, $CDCl_3$, δ): 173.3, 170.4 (CO), 161.3, 147.0 (C4 Ar), 134.2, 124.3, 114.7, 114.6 (=C-H), 74.7, 67.9, 61.3 (CH_2-O), 36.9 (CH_2-N), 33.9, 28.8 (CH_2), 28.3 (CH), 25.6, 24.4, 19.2 (CH_3) ppm. MALDI-TOF MS (matrix: dithranol, m/z): 508.3 $[M-H]^+$, 530.4 $[M-Na]^+$.Anal. Calcd for $C_{28}H_{33}N_3O_6$: C 66.26, H 6.55, N 8.28; found: C 66.21, H 6.83, N 8.22.

*Synthesis of (***5***)*: The protected maleimide (**1**) (1.2 g, 5.7 mmol), isopropylidene-2,2-bis(methoxy)propionic acid (1.2 g, 6.9 mmol) and 4-(dimethylamino)pyridinium 4-toluenesulfonate (DPTS) (1.7 g, 5.7 mmol) were dissolved in dichloromethane (50 mL). The reaction flask was flushed with argon, and *N,N′*-dicyclohexylcarbodiimide (DCC) (2.2 g, 7.4 mmol) was added. The mixture was stirred at ambient temperature for 24 h under argon atmosphere. The white precipitate formed was filtered off, and the solvent was evaporated. The crude product was purified by flash column chromatography on silica gel and eluted with 7:3 ethyl acetate/dichloromethane. The target product was obtained as a yellow powdery solid. Yield: 80%. IR (KBr): ν = 1772, 1723, 1698 (C=O), 1279, 1247(C-O). ^{1}H NMR (400 MHz, $CDCl_3$, δ): 6.51 (t, J = 1.0 Hz, 2H, = C-H), 5.26 (t, J = 1.0 Hz, 2H, CH), 4.32-4.27 (m, 2H, CH_2-OCO), 4.13 (d, J = 11.8 Hz, 2H, -HC*H*-O), 3.83–3.73 (m, 2H, CH_2-N), 3.58 (d, J = 11.8 Hz, 2H *H*CH-O), 2.86 (s, 2H, CH), 1.40 (s, 3H, CH_3), 1.37 (s, 3H, CH_3), 1.18 (s, 3H, CH_3) ppm. ^{13}C NMR (100 MHz, $CDCl_3$, δ): 175.8, 173.8 (CO), 136.4 (=C-H), 97.9 (C4), 80.7 (CH-O), 65.7, 61.1 (CH_2-O), 47.4 (CH), 41.6 (C4), 37.7(CH_2-N), 23.8, 23.2, 18.4 (CH_3) ppm.

*Synthesis of (***6***)*: DOWEX-50-X2 resin (0.1 g) was added to a solution of compound (**5**) (0.5 g, 1.5 mmol) in methanol (15 mL). The mixture was stirred for 3 h at ambient temperature. Subsequently, the resin was filtered off and the solvent removed under vacuum to give (**6**) as a colorless viscous oil. Yield: 90%. IR (KBr): ν = 3500 (O-H), 1772, 1721, 1699 (C=O), 1279, 1246 (C-O). ^{1}H NMR (400 MHz, $CDCl_3$, δ): 6.45 (t, J = 1.0 Hz, 2H, =C-H), 5.22 (t, J = 1.0 Hz, 2H, CH), 4.32–4.19 (m, 2H, CH_2-OCO), 3.75-3.69 (m, 4H, CH_2-O), 3.64-3.60 (m, 2H, CH_2-N), 2.83 (s, 2H, CH), 2.81 (t, J = 6.8 Hz, 1H, OH), 0.97 (s, 3H, CH_3) ppm. ^{13}C NMR (100 MHz, $CDCl_3$, δ): 175.8, 173.8 (CO), 136.4 (=C-H), 80.7 (CH-O), 65.7, 61.1 (CH_2-O), 47.4 (CH), 41.6(C4), 37.7 (CH_2-N), 18.4 (CH_3) ppm.

*Synthesis of (***7***)*: After in situ preparation of the the acid chloride derivate of 6-[4-(4′-isobutyloxyphenylazo)phenyloxy] hexanoic acid (**2**) (1.0 g, 2.4 mmol), it was added to a solution of compound **6** (0.4 g, 1.1 mmol) and triethylamine (0.2 g, 2.4 mmol) in 20 mL of dichloromethane. The mixture was stirred for 3 h at ambient temperature under argon atmosphere. After this time, the precipitate was filtered off and the solvent removed under vacuum. The white precipitate formed was filtered off, and the solvent was evaporated. The crude product was purified by flash column chromatography on silica gel and eluted with 7:3 ethyl acetate/dichloromethane. Yield: 65%. IR (KBr): ν = 1739, 1703 (C=O), 1601, 1581, 1498 (Ar), 1243, 1149, 1024 (C-O), 843 (Ar). ^{1}H NMR (400 MHz, $CDCl_3$, δ): 7.90-7.86 (m, 8H, Ar H), 6.96-6.90 (m, 8H, Ar H), 6.48 (t, J = 1.0 Hz, 2H, =C-H), 5.29 (t, J = 1.0 Hz, 2H, CH), 4.26-4.08 (m, 6H, CH_2-OCO), 4.01 (t, J = 6.4 Hz, 4H, CH_2-OPh), 3.82-3.73 (m, 6H, CH_2-O, CH_2-N), 2.86 (s, 2H, CH), 2.35 (t, J = 7.4 Hz, 4H, CH_2-CO), 2.10-2.03 (m, 2H, CH), 1.86-1.75 (m, 4H, CH_2), 1.73-1.64 (m, 4H, CH_2), 1.54-1.44 (m, 4H, CH_2), 1.22 (s, 3H, CH_3), 1.05 (d, J = 6.7 Hz, 12H, CH_3) ppm. ^{13}C NMR (100 MHz, $CDCl_3$, δ): 175.9, 172.9, 172.3 (C=O), 161.9, 160.9, 146.8, 146.8 (C4 Ar), 136.4, 124.1, 114.6, 114.5 (=C-H), 80.7 (CH-O), 74.6, 67.8, 64.9, 61.4 (CH_2-O), 47.4 (CH), 46.2 (C4), 37.6 (CH_2-N), 33.8, 28.8 (CH_2), 28.2 (CH), 25.5, 24.5(CH_2), 19.2, 17.5 (CH_3) ppm.

*Synthesis of (***8***)*: The protected maleimide (**7**) was suspended in 150 mL toluene and heated to reflux. The reaction was monitored by TLC. After 4 h, the solvent was removed under reduced pressure to give (**8**) as a yellow powder. Yield (95%). IR (KBr): ν = 1731, 1713 (C=O), 1601, 1582, 1498 (Ar), 1243, 1149, 1034 (C-O), 845 (Ar). ^{1}H NMR (400 MHz, $CDCl_3$, δ): 7.90-7.86 (m, 8H, Ar H), 6.96-6.90 (m, 8H, Ar H), 6.70 (s, 2H, =C-H), 4.27-4.12 (m, 6H, CH_2-OCO), 4.01 (t, J = 6.4 Hz, 4H, CH_2-OPh), 3.82-3.73 (m, 6H, CH_2-O, CH_2-N), 2.35 (t, J = 7.4 Hz, 4H, CH_2-CO), 2.10-2.03 (m, 2H, CH), 1.86-1.75 (m, 4H, CH_2), 1.73-1.64 (m, 4H, CH_2), 1.54-1.44 (m, 4H, CH_2), 1.22 (s, 3H, CH_3), 1.05 (d, J = 6.7 Hz, 12H, CH_3) ppm. ^{13}C NMR (100 MHz, $CDCl_3$, δ): 172.9, 172.3, 170.3 (CO), 161.9, 160.9, 146.8, 146.8 (C4 Ar), 134.2, 124.1, 114.6, 114.5 (=C-H), 74.6, 67.8, 64.9, 61.4 (CH_2-O), 46.2 (C4), 37.6 (CH_2-N), 33.8, 28.8 (CH_2), 28.2 (CH), 25.5, 24.5 (CH_2), 19.2, 17.5 (CH_3) ppm. MALDI-TOF MS (matrix: dithranol, m/z): 990.6 $[M\text{-}H]^+$, 1012.5 $[M\text{-}Na]^+$. Anal calcd for $C_{55}H_{67}N_5O_{12}$: C 66.72: H 6.82: N 7.07; found: C 66.53: H 7.01: N 7.05.

Activation of Silicon Wafers: Prior to surface activation, the silicon wafers (p-type, boron doped (100) from Si-Mat Silicon Materials, Landsberg, Germany) were cleaned with chloroform, acetone and ethanol. The wafers were rinsed thoroughly with fresh solvent and sonicated 5 min several times with each solvent. After cleaning, the silicon wafers were activated by immersion in Piranha solution (H_2SO_4 95%/H_2O_2 35% 3:1 vol/vol) at 90 °C for 1 h. *Caution: piranha solution is an extremely strong oxidant!* After extensive rinsing with deionized water, they were dried under a stream of argon.

Functionalization of Silicon Wafers with Tetrazole (TET): The activated silicon wafers were placed in a flask containing a solution of silane-functionalized tetrazole (**9**) in dry toluene (4.8 mg in 1 mL). The flask was heated to 50 °C overnight. Subsequently, the wafers were rinsed thoroughly with fresh toluene as well as chloroform and sonicated for 5 min. The wafers were finally dried in a stream of argon.

Functionalization of Silicon Wafers with Azobenzene (AZO1 and AZO2): The tetrazole functionalized silicon wafers were placed in a quartz flask containing an azobenzene solution. The flask was introduced into a photoreactor with two lamps emitting between 290 and 315 nm and irradiated for a pre-set time interval. Subsequently the wafers were rinsed thoroughly with fresh chloroform and sonicated for 5 min. The wafers were finally dried in a stream of argon.

Photoisomerization of Azobenzene Functionalized Silicon Wafers: The azobenzene functionalized silicon wafers were introduced in a photoreactor with two lamps (310–400 nm) for 30 min. After this time, the wafers were kept in the dark.

Characterization Techniques: *IR* spectra were obtained on a Nicolet Avatar 360-FT-IR spectrometer using KBr pellets. NMR spectra were measured on a Bruker AV-400 spectrometer. Elemental analyses were performed using a Perkin–Elmer 2400 microanalyzer. Mass spectra were recorded on an Autoflex mass spectrometer (Bruker Daltonics) and a LXQ mass spectrometer (ThermoFisher Scientific) equipped with an atmospheric pressure ionization source operating in the nebulizer-assisted electrospray mode. The instrument was calibrated in the m/z range 195-1822 using a standard comprising caffeine, Met-Arg-Phe-Ala acetate (MRFA), and a mixture of fluorinated phosphazenes (Ultramark 1621, all from Aldrich). MALDI-TOF MS was performed on an Autoflex mass spectrometer (Bruker Daltonics). XPS measurements were performed using a K-Alpha XPS spectrometer (ThermoFisher Scientific, East Grinstead, UK). All samples were analyzed using a microfocused, monochromated Al Kα X-ray source (400 µm spot size). The kinetic energy of the electrons was measured by a 180° hemispherical energy analyzer operated in the constant analyzer energy mode (CAE) at 50 eV pass energy for elemental spectra. Data acquisition and processing using the Thermo Avantage software is described elsewhere.[37] The spectra were fitted with one or more Voigt profiles (binding energy uncertainty: ± 0.2 eV). The analyzer transmission function, Scofield sensitivity factors,[38] and effective attenuation lengths (EALs) for photoelectrons were applied for quantification. EALs were calculated using the standard TPP-2M formalism.[39] All spectra were referenced to the C1s peak of hydrocarbon at 285.0 eV binding energy controlled by means of the well known photoelectron peaks of metallic Cu, Ag, and Au, respectively. ToF-SIMS[40,41] was performed on a TOF.SIMS5 instrument (ION-TOF GmbH, Münster, Germany), equipped with a Bi cluster liquid metal primary ion source and a non-linear time of flight analyzer. UHV base pressure was $<5 \times 10^{-9}$ mbar. The Bi source was operated in the bunched mode providing 1.1 ns Bi^{1+} ion pulses at 25 keV energy and a lateral resolution of approx. 4 µm. The short pulse length allowed for high mass resolution to analyze the complex mass spectra of the immobilized organic layers. Images larger than the maximum deflection range of the primary ion gun of 500×500 µm^2 were obtained using the manipulator stage scan mode. Spectra were calibrated on the C^-, C_2^-, C_3^-, or on the C^+, CH^+, CH_2^+, and CH_3^+ peaks. Primary ion doses were kept below 10^{11} ions/cm^2 (static SIMS limit). Advancing and receding contact angle measurements were performed with an OCA5 instrument (dataphysics, Filderstadt, Germany). HPLC grade water was used and all measurements were performed on several spots of the substrate and averaged ($n > 3$). The photoconjugation reaction was carried out with compact low-pressure fluorescent lamps Philips PL-S 9W/12 emitting UV irradiation between 290 and 315 nm. Solution tests were also performed with a hand-held UV lamp and OSRAM Puritec HNS L 36 W lamps emitting at 254 nm. The azobenzene photoisomerization was performed with compact low-pressure fluorescent lamps Philips CLEO PL-L 36W emitting between 310 and 400 nm (λ_{max} = 355 nm).

Supporting Information

Supporting Information is available from the Wiley Online Library or from the author.

Acknowledgements

The current work was supported by the MINECO, Spain, under the project MAT2011-27978-C02-01, Fondo Europeo de Desarrollo Regional (FEDER) and Gobierno de Aragon. E. B. acknowledges the CSIC JAE-Pre contract funding her PhD studies. C.B.-K. acknowledges continued funding from the Karlsruhe Institute of Technology (KIT), the German Research Council (DFG) as well as the ministry of science and arts of the state of Baden-Württemberg.

Received: December 5, 2012
Revised: January 31, 2013
Published online: March 12, 2013

[1] T. P. Russell, *Science* **2002**, *297*, 964.
[2] T. L. Sun, L. Feng, X. F. Gao, L. Jiang, *Acc. Chem. Res.* **2005**, *38*, 644.
[3] M. Grunze, *Science* **1999**, *283*, 41.
[4] K. Ichimura, S. K. Oh, M. Nakagawa, *Science* **2000**, *288*, 1624.
[5] D. Gustina, E. Markava, I. Muzikante, B. Stiller, L. Brehmer, *Adv. Mater. Opt. Electron.* **1999**, *9*, 245.
[6] A. P. Wu, D. R. Talham, *Langmuir* **2000**, *16*, 7449.
[7] M.-M. Russew, S. Hecht, *Adv. Mater.* **2010**, *22*, 3348.
[8] S. K. Oh, M. Nakagawa, K. Ichimura, *J. Mater. Chem.* **2002**, *12*, 2262.
[9] N. Delorme, J. F. Bardeau, A. Bulou, F. Poncin-Epaillard, *Langmuir* **2005**, *21*, 12278.
[10] F. Hamelmamm, U. Heinzmann, U. Siemling, F. Bretthauer, J. V. der Bruggen, *Appl. Surf. Sci.* **2004**, *222*, 1.
[11] X. Liu, M. Cai, Y. Liang, F. Zhou, W. Liu, *Soft Matter* **2011**, *7*, 3331.
[12] H. S. Lim, W. H. Lee, S. G. Lee, D. Lee, S. Jeon, K. Cho, *Chem. Commun.* **2010**, *46*, 4336.
[13] J. R. Silva, F. F. Dall'Agnol, O. N. Oliveira, J. A. Giacometti, *Polymer* **2002**, *43*, 3753.

[14] a) J. Razna, P. Hodge, D. West, S. Kucharski, *J. Mater. Chem.* **1999**, *9*, 1693; b) J. Gu, H. Lü, L. Liu, B. Liang, Y. Chen, Z. Lu, *Supramol. Sci.* **1998**, *5*, 675.
[15] R. H. El Halabieh, O. Mermut, C. J. Barrett, *Pure Appl. Chem.* **2004**, *76*, 1445.
[16] P. Uznanski, J. Pecherz, *J. Appl. Polym. Sci.* **2002**, *86*, 1459.
[17] M. Han, K. Ichimura, *Macromolecules* **2000**, *34*, 90.
[18] R. M. Arnold, N. E. Huddleston, J. Locklin, *J. Mater. Chem.* **2012**, *22*, 19357.
[19] a) H. C. Kolb, M. G. Finn, K. B. Sharpless, *Angew. Chem. Int. Ed.* **2001**, *40*, 2004; b) C. Barner-Kowollik, F. E. Du Prez, P. Espeel, C. J. Hawker, T. Junkers, H. Schlaad, W. Van Camp, *Angew. Chem. Int. Ed.* **2011**, *50*, 60.
[20] a) T. Pauloehrl, G. Delaittre, V. Winkler, A. Welle, M. Bruns, H. G. Börner, A. M. Greiner, M. Bastmeyer, C. Barner-Kowollik, *Angew. Chem. Int. Ed.* **2012**, *51*, 1071; b) B. J. Adzima, Y. Tao, C. J. Kloxin, C. A. DeForest, K. S. Anseth, C. N. Bowman, *Nat. Chem.* **2011**, *3*, 256.
[21] M. Dietrich, G. Delaittre, J. P. Blinco, A. J. Inglis, M. Bruns, C. Barner-Kowollik, *Adv. Funct. Mater.* **2012**, *22*, 304.
[22] T. D. Pauloehrl, Guillaume, M. Bruns, M. Meißler, H. G. Börner, M. Bastmeyer, C. Barner-Kowollik, *Angew. Chem. Int. Ed.* **2012**, *51*, 9181.
[23] J. S. Clovis, A. Eckell, R. Huisgen, R. Sustmann, *Chem. Ber.* **1967**, *100*, 60.
[24] W. Song, Y. Wang, J. Qu, M. M. Madden, Q. Lin, *Angew. Chem. Int. Ed.* **2008**, *47*, 2832.
[25] a) Y. Z. Wang, W. J. Hu, W. J. Song, R. K. V. Lint, Q. Lin, *Org. Lett.* **2008**, *10*, 3725; b) Y. Z. Wang, C. I. R. Vera, Q. Lin, *Org. Lett.* **2007**, *9*, 4155.
[26] X. Tong, G. Wang, A. Soldera, Y. Zhao, *J. Phys. Chem. B.* **2005**, *109*, 20281.
[27] a) H. Meier, H. Heimgartner, *Helv. Chim. Acta* **1985**, *68*, 1283; b) V. Lohse, P. Leihkauf, C. Csongar, G. Tomaschewski, *J. Prakt. Chem.* **1988**, *330*, 406; c) R. Darkow, M. Yoshikawa, T. Kitao, G. Tomaschewski, J. Schellenberg, *J. Polym. Sci., Part A: Polym. Chem.* **1994**, *32*, 1657; d) G. Bertrand, C. Wentrup, *Angew. Chem. Int. Ed.* **1994**, *33*, 527; e) D. Moderhack, *J. Prakt. Chem.* **1998**, *340*, 687; f) J. Wang, W. Zhang, W. Song, Y. Wang, Z. Yu, J. Li, M. Wu, L. Wang, J. Zang, Q. Lin, *J. Am. Chem. Soc.* **2010**, *132*, 14812; g) W. Song, Y. Wang, J. Qu, Q. Lin, *J. Am. Chem. Soc.* **2008**, *130*, 9654; h) Y. Wang, W. Song, W. J. Hu, Q. Lin, *Angew. Chem. Int. Ed.* **2009**, *48*, 5330; i) M. M. Madden, C. I. Rivera Vera, W. Song, Q. Lin, *Chem. Commun.* **2009**, 5588.
[28] C. De Marco, S. M. Eaton, R. Suriano, S. Turri, M. Levi, R. Ramponi, G. Cerullo, R. Osellame, *ACS Appl. Mater. Interfaces* **2010**, *2*, 2377.
[29] E. H. Lock, D. Y. Petrovykh, P. Mack, T. Carney, R. G. White, S. G. Walton, R. F. Fernsler, *Langmuir* **2010**, *26*, 8857.
[30] E. Szocs, I. Bakó, T. Kosztolányi, I. Bertóti, E. Kálmán, *Electrochim. Acta* **2004**, *49*, 1371.
[31] P. G. Rouxhet, A. M. Misselyn-Bauduin, F. Ahimou, M. J. Genet, Y. Adriaensen, T. Desille, P. Bodson, C. Deroanne, *Surf. Interface Anal.* **2008**, *40*, 718.
[32] M. Strobel, C. S. Lyons, *Plasma Process. Polym.* **2011**, *8*, 8.
[33] Y. L. Chen, C. A. Helm, J. N. Israelachvili, *J. Phys. Chem.* **1991**, *95*, 10736.
[34] L. M. Siewierski, W. J. Brittain, S. Petrash, M. D. Foster, *Langmuir* **1996**, *12*, 5838.
[35] N. Delorme, J. F. Bardeau, A. Bulou, F. Poncin-Epaillard, *Langmuir* **2005**, 21.
[36] G. Mantovani, F. Lecolley, L. Tao, D. M. Haddleton, J. Clerx, J. J. L. M. Cornelissen, K. Velonia, *J. Am. Chem. Soc.* **2005**, *127*, 2966.
[37] K. L. Parry, A. G. Shard, R. D. Short, R. G. White, J. D. Whittle, A. Wright, *Surf. Interface Anal.* **2006**, *38*, 1497.
[38] J. H. Scofield, *J. Electron Spectrosc. Relat. Phenom.* **1976**, *8*, 129.
[39] S. Tanuma, C. J. Powell, D. R. Penn, *Surf. Interface Anal.* **1994**, *21*, 165.
[40] G. J. Leggett, J. C. Vickerman, *Annu. Rep. Prog. Chem., Sect. C* **1993**, *88*, 77.
[41] H. F. Arlinghaus, *Appl. Surf. Sci.* **2008**, 1058.